Thesis Presented to the College of Engineering
of the University of Florida in Partial Fulfillment of the
Requirements for Graduation with Highest Honors

Parametric Study on the use of Hoberman Mechanisms for Small Satellite Reconfigurable Solar and Antenna Arrays

By

Katherine Ann Faist

May 2010

Chair: Gloria Wiens
Department: Mechanical and Aerospace Engineering

One of the primary concerns associated with the design of small satellites is achieving power capacities sufficient to support payload and mission operations while simultaneously retaining communications capabilities. Furthermore, small satellites must be able to easily transform from their tightly stowed configurations to their fully operational mode. To address these concerns, this thesis presents the modeling and analysis of a class of foldable mechanisms, based on the Hoberman mechanism's kinematic theory, and their parametric coupling with the system parameters of both an antenna array and a solar array. The resulting models provide viable solar array and antenna array designs to generate power and communications capabilities on small satellites.

Using a combination of theoretical, graphical and numerical techniques, measures of array performance are calculated and presented in terms of the geometric and operational aspects of the deployable mechanism forming the backbone structure of the

array. To gauge the comparative performance of the Hoberman based mechanism designs, the same performance measures (deployable size, power, stowed volume, ballistic drag, gain and actuation) are calculated for the current state-of-the-art solar arrays. From the analysis, projected surface area and corresponding ballistic drag factor calculations indicate that the Hoberman solar array design will have a longer orbital life than the current state-of-the-art of fold out panel designs. This greater orbital life capability is compounded when considering 136% increase in surface area for power generation using the Hoberman based design compared to the 100% with the CUTE-1 fold out panel. Another attribute of the Hoberman-based design is that it only has a single degree-of-freedom. Furthermore, its geometric configuration offers deployments that impart minimal torque and shaking force on the small satellite, making this design preferable for missions with a high degree of attitude sensitivity. However, in general, the specific Hoberman-based power generation concept selection will remain dependent on the given orbit parameters.

In summary, the deployable nature of the single degree-of-freedom Hoberman mechanisms makes them viable alternatives to the current multiple degree-of-freedom deployable systems. The power generation capability of the deployable solar array has been demonstrated to yield a significant improvement over current methods of power generation for small satellites. In addition, the deployable dish design allows for enhanced communications capabilities while saving valuable stowage space.

ACKNOWLEDGMENTS

I would like to extend my sincere gratitude to the many people who helped me pursue my educational goals. I am most thankful to God, to whom I owe my existence, my abilities, and my purpose in life. I am immensely indebted to my parents, Jim and Barbara Faist, who constantly encouraged me and supported me throughout my entire academic experience. Appreciation is extended to my advisor, Dr. Gloria Wiens, who provided valuable input and guidance throughout this research process. I would also like to thank my fellow SSMG members, Shawn Miller and Jimmy Roark, for their technical support. I would like to acknowledge my supervisory committee members: Dr. Janise McNair and Dr. Carl D. Crane. Thank you for your expertise and assistance.

Funding was made possible by Lockheed Martin, Grant No. RRMJS6769. Partial funding was also provided by the University of Florida's University Scholars Program. Use of critical software packages, SolidWorks and Adams, was provided by the University of Florida for educational purposes.

LIST OF FIGURES

LIST OF TABLES

Page

TABLE OF CONTENTS

Page

Part 1: Introduction

There is a new research focus within the world of commercial and government satellites towards miniaturization. While large satellites are currently used for many applications from GPS to satellite radio, some application areas are beginning to see the benefit of small satellites. Small satellites are relatively inexpensive to build and to fly, and they are incredibly versatile in their uses. Furthermore, the currently used picosatellite CubeSat design enables collections of small satellite cubes to lock together in user-specified formations, resulting in a broad array of potential uses for these cubes, beyond the single cube. However, the functionality of the CubeSat design is limited by the small amount of volume that each cube can contain. If each cube is required to carry a payload, then the available space for internal power generation and communications arrays is incredibly minute. Within the SmallSat community, the 1U form-factor of the CubeSat is defined to be 10cm by 10cm by 10 cm. Pumpkin Inc. has secured dominance in the market with its 1U and 3U kits (see Figure 1) that are compatible with the P-pod launch platforms widely used by academe.

The current practice is to attach non-moving solar panels and/or hinged panels to the sides of the CubeSat [4]. While this existing solution is simple to implement, using a foldable mechanism, deployable with a single degree of freedom, to increase the satellite surface area exposed to the sun should dramatically improve power generation while providing ease of actuation. In addition, these foldable mechanisms can be used as deployable and reconfigurable antenna dishes which offer the small satellite capabilities to maximize antenna gain when in its operational mode and to remain within the stowed space limitations when in its launch configuration. To gauge the potential impact of foldable mechanisms on the CubeSat technology, there is a need to further develop, characterize and quantify the scope of these new deployable structures being developed for the CubeSat.

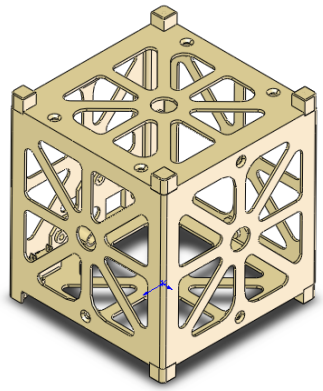

Figure 1: CubeSat Pumpkin kit, single unit (The CubeSat Kit 3D CAD models are © Copyright Pumpkin, Inc. All rights reserved worldwide.)

In this thesis, the application of these mechanisms is to maximize power generation by increasing the external surface area of the cube that is available for solar panel mounts and when in its stowed configuration to allow the packaging of these

components into a small volume. Antenna array packaging and mechanical reconfigurability are also key points of research interest that are linked with the power generation research where the goal is to maximize the achievable gainof the antenna. The Hoberman mechanism's kinematic theory has been found to provide radial motion of joints driven by two circumferentially actuated rings, as illustrated in Figure 2 [1]. For both the solar panel design and the parabolic and spherical antenna designs presented in this thesis, the radial motion of the joints is considered key to developing the reconfigurability aspect of the antenna array as well as the extendibility of the solar panels. Furthermore, this Hoberman-based design approach allows for the use of counter-rotating rings to drive the solar panels outward, minimizing the impact of the actuation torque on the satellite's attitude.

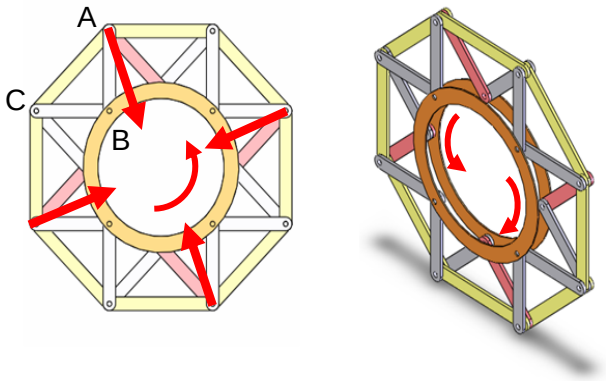

Figure 2. Planar Hoberman radially foldable mechanisms – fully deployed.

Objective

To provide small satellites greater power capacity and communication capabilities, research is needed for investigating, the relationships between the kinematics of foldable and deployable mechanisms and the practical applications in the world of small satellite power generation and communications. To address this need, this thesis presents the modeling and analysis of a class of foldable mechanisms, based on the Hoberman mechanism's kinematic theory, and their parametric coupling with the system parameters of both an antenna array and a solar array. The objective is not only to enable greater operational functionality and capacity, but to create a class of small satellites that can easily transform from their tightly stowed configurations to their fully operational mode. After first elaborating on the characteristics of the Hoberman mechanism that make it well-suited for application in deployable solar array and antenna mechanisms, the goal is to identify key mechanism parameters and demonstrate in the analysis their impact on the array performance and the viability of the design.

Current Technologies

The need for increased power on pico- and nano- satellites will become more critical as the payloads and instrumentation capabilities improve. These small satellites

are starting to utilize more powerful payloads such as attitude control and determination systems that require up to 5 Watts of power to operate. The majority of picosatellites and nanosatellites today are limited in capabilities due to the small amount of power available for the mission. The typical 1U CubeSat can supply approximately 1.5-2 Watts using GaAs solar panels, weighs approximately 1 kg, and is 10 cm by 10 cm by 10 cm. This power generation is limited by the surface area of less than 100 cm^2 per side of the cube and the efficiencies of the solar panels (~ 26%). In order to run an attitude control system on a CubeSat, the satellite fully charges the batteries, shuts down non-essential systems, and runs in a power negative configuration for maneuvering. Using a deployable mechanism to increase the total surface area exposed to the sun can significantly increase the available power for the mission while maintaining the same overall size requirements for launch. This will reduce the need for either running in a power negative mode or shutting down nonessential systems thus enabling a more efficient and capable mission. By developing a deployable mechanism for this use, the technology may also be utilized as a base technology for new, reconfigurable antenna designs leading to more powerful and useful pico and nano-satellite missions.

Deployable solar arrays that are currently used on CubeSats include folding panels such as those used on the CUTE I [8]. The CUTE I design makes use of an entire side of the satellite folding out, actuated by a spring loaded hinge. To hold the solar array in place during launch, a paddle stopper holds the panel down. This is connected to a vacuum motor that removes the stopper when the panel is deployed. However, the movement of the motor and the panel deployment may cause a severe change in attitude and cause a similar design on a CubeSat to tumble. This would be unacceptable on a satellite that requires attitude control. With the same type of folding panels, the MOVE CubeSat from The Technical University of Munich uses a similar deployment, but with a type of pyro-cutter to activate the deployment [9].

Most current small satellites use the UHF or the VHF range of frequencies for communication. The University of Hawaii has proposed using a grid oscillator antenna for use at high frequencies [10]. These antennas have a grid of embedded circuitry mounted in front of a radiating surface. The benefits of using this type of antenna include higher data transfer rates in a low profile, rectangular structure. It is also more compact than array antennas at high frequencies. When attached to a frame, this type of antenna will not need to be deployed to operate. However, there are drawbacks to operating at higher frequency, including greater power consumption. In addition, this type of antenna requires space on the side of the cube, sacrificing solar arrays for communication purposes. The space needed on the cube would be a 5cm by 7cm rectangle. The omni-directional radiation pattern of this antenna also results in wasted energy, which could be prevented by the directional antenna dish proposed in this thesis. On a CubeSat with attitude control, advantages can also be gained by using a directional antenna, such as the Yagi-Uda antenna shown in Figure 3. Gains in these antennae are higher, and they consume less power. Signals received have a better signal to noise ratio due to the directional properties of the antenna. To provide a physical scale of a possible Yagi-Uda antenna dimension for a small satellite, a typical wavelength is 0.125 m which corresponds to overall antenna dimensions of 6.86cm x 2.49 cm.

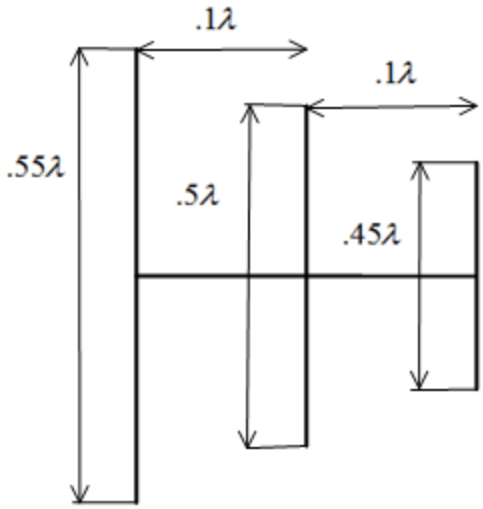

Figure 3: Yagi-Uda antenna configuration (drawing is not drawn to scale)

Part 2: Solar Panel Array Design

Solar Array Theoretical Development

The Hoberman mechanism provides a radially foldable structure that can be used to support space structures for small satellites. Figure 4 illustrates a Hoberman-based solar array configuration mounted on a 1U small satellite, which is the solar array focus of this thesis. Previously conducted research [1, 2, 3] has used the algebraic locus of the coupler curve of a theoretically equivalent prismatic-revolute-revolute-prismatic (PRRP) linkage to create a circumferentially actuated foldable mechanism consisting of only revolute (R) joints, as was shown in Figure 2. For notation, the P corresponds to a prismatic joint and R corresponds to a revolute joint in each of the closed-loop kinematic linkages coupled within the Hoberman mechanism. The order of the P and R denotes the sequence of the joints within the linkage.

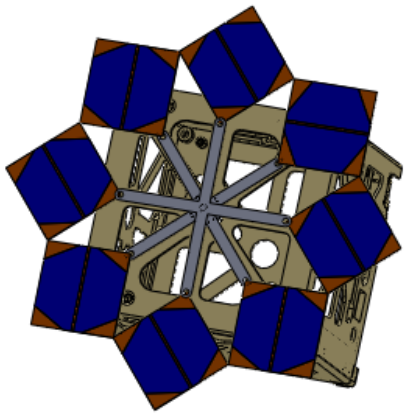

Figure 4: Deployed mechanism mounted on a CubeSat 1U form-factor.

In Figure 2, the planar Hoberman consists of two actuation rings, each in a parallel plane, and a series of binary links. When the rings are rotated counter to each other, one in the clockwise direction and the other in the counter-clockwise direction, the binary links are drawn in radially towards the center of the rings as the mechanism contracts. Figure 2 shows the mechanism fully deployed. Figure 5 demonstrates that the binary links may be combined to form a single ternary link ABC, denoted as a leaf [1, 2, 3]. In the solar array application, the ternary link is extended to a square dimension (ABCF) with n=8 yielding $\alpha=(\pi/4)$. The corners A and C of the leaves form the joints of an equivalent PRRP linkage. The motion of points A and C are constrained to lie on the x axis and a line defined by the angle α, respectively. This constrained radial-translational motion corresponds to motion within the equivalent prismatic joints of the PRRP linkage. Per reference [1], the governing equation of the coupler curve of point B is as follows, where n is the number of leaves in the design, the r's are the geometric dimensions of the links as shown in Figure 5, and (x,y) are the position coordinates of point B.

$$a_1 x^2 + a_2 y^2 + a_3 xy + a_4 = 0$$

$$a_1 = r_1^{\,2} \tan^2 \alpha + r_2^{\,2} \tan^2 \alpha$$

$$a_2 = r_2^{\,2} \tan^2 \alpha + r_3^{\,2} \tan^2 \alpha + 2r_1 r_2 \tan \alpha + 2r_2 r_3 \tan \alpha + r_1^2 + r_3^{\,2} + 2r_1 r_3$$

$$a_3 = -2(r_1 r_2 \tan^2 \alpha + r_2 r_3 \tan^2 \alpha + r_1^2 \tan \alpha + r_1 r_3 \tan \alpha)$$

$$a_4 = -2r_2^3 r_3 \tan \alpha - r_2^2 r_1^2 - r_3^2 r_1^2 \tan^2 \alpha - 2r_1 r_2^3 \tan \alpha - 2r_1 r_2^2 r_3 - r_2^4 \tan^2 \alpha + 2r_1^2 r_2 r_3 \tan \alpha + 2r_1 r_2^2 r_3 \tan^2 \alpha$$

$$\alpha = \frac{2\pi}{n}$$

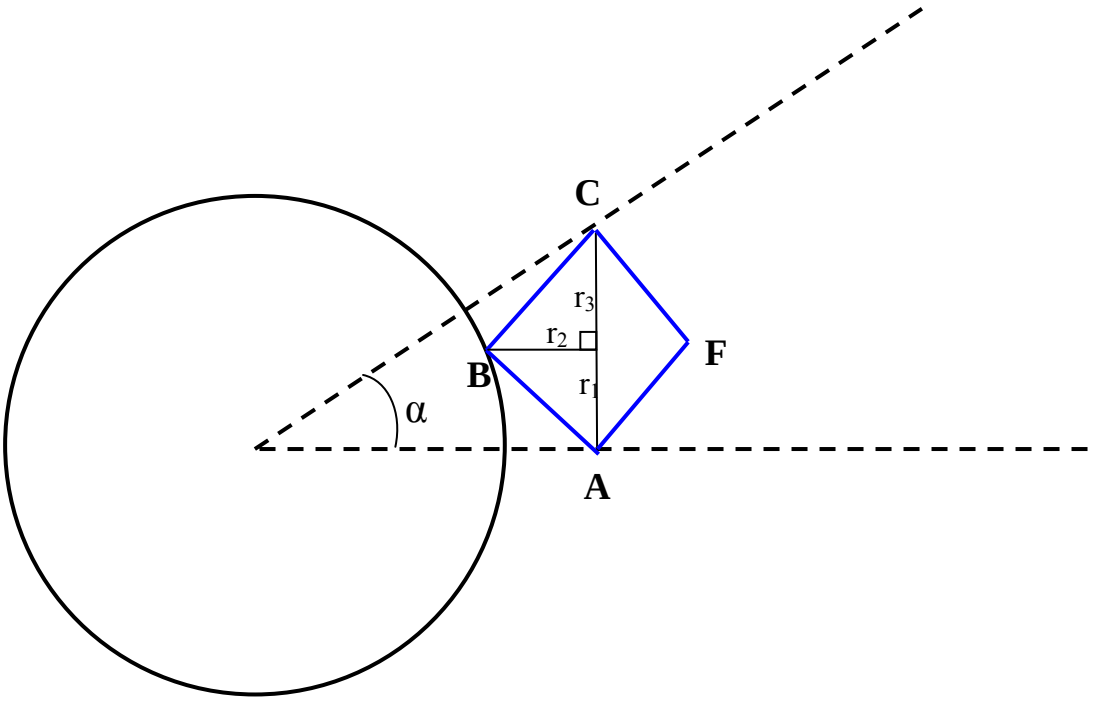

Figure 5. Leaf formation from 4 interconnected binary links. Points A and C motion can be denoted as P joints. The links that form leaves are ABCF, and similarly ADE for adjacent leaf in mechanism chain.

When one selects the geometric parameters such that $a_1 = a_2$ and $a_3 = 0$, the coupler curve of point B traces along the circumference of a circle. This allows point B to attach to the circumferentially actuatable rings, driving the entire mechanism. Imposing these two conditions on the coupler curve equation, one obtains the following relationships between r_1, r_2 and r_3 where the depiction in Figure 5 has already incorporated r_2 being negative in value relative to r_1 and r_3.

$$r_2 = -\frac{r_1}{\tan\alpha}$$

$$r_1 = r_3$$

Figure 6 [2] shows the deployment of the mechanism with the solar panels attached to the leaves and the two rings replaced with two spokes rotating about concentric axes at the center of the mechanism. From left to right, Figure 6 shows the state of the mechanism for a rotation angle of 0°, 45°, 90°, and 135°. When the mechanism is actuated to 135°, it is fully open. However, the actual implementation of the mechanism will only need to open the deployable to the 90° angle where the interior square opening will be filled with solar panel.

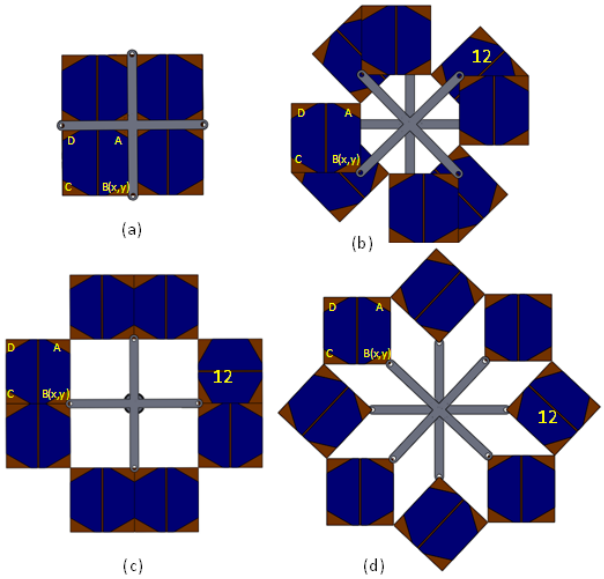

Figure 6. Deployment states of the mechanism shown for relative input rotation angles, a. 0°, b. 45°, c. 90°, and d. 135°.

Heterogeneous link design

Although it is preferable that all the link sizes be homogenous for the sake of simplicity, this is not a necessary condition for mobility. In a heterogeneous design, the various values of the α's need not all be the same, but they must all add up to 360° in order to attain circumferential actuation [1]. Aside from varying link sizes, another case of a heterogeneous design is one in which the leaves are not square. The extent of contraction of the homogeneous design is only limited by the fact that a revolute joint may not in reality be infinitesimally small. When the mechanism is in the stowed position, the joints at points A and C must have a volume of zero in order to fully contract the mechanism without an interference fit. An infinitesimally small joint size will lead to complete contraction, so that the area of the interior polygon enclosed by the joints is equal to zero.

In addition, the extent of contraction of the heterogeneous design is limited not necessarily by varying values of α, but by the shape of the leaves themselves. As the difference in the lengths of sides AD and CD (Figure 5) increases from a nominal value of 0, the foldability of the design decreases [1]. In other words, if the square ABCD is made into a rectangle whose width is much shorter than its length, the foldability would drastically decrease.

Other Designs

It is possible to change the number of leaves in the design while still maintaining the circumferential actuation and single degree-of-freedom system [4]. The impact of this is dicussed in the following section. In all such Hoberman-based designs and as illustrated in Figure 6, solar panels may be attached to each leaf, resulting in the design of a deployable solar array. Furthermore, optimizing the geometry of the leaves with the application, this single degree-of-freedom system has vast potential for new innovative configurations.

Solar Array Performance Analysis

In this section using graphical, analytical and/or numerical methods, various measures of performance are determined and discussed to quantify the overall viability of using the Hoberman-based deployable solar array mechanism design compared to the state-of-the-art for small satellite solar array systems. These are tabulated in Table 1 showing a comparison between small satellite designs. Figure 7 shows the three 1U solar array designs and the baseline CubeSat design with no deployable for which the performance analysis was conducted.

(a) baseline design **(b) CUTE-1 fold-out [7]** **(c) circumferentially actuated** **(d) Four-panel fold-out [4]**

Figure 7. CubeSat 1U deployable solar arrays and baseline design.

First, looking at the surface area achievable for the solar arrays, it is found that using the circumferentially actuated Hoberman design resulted in an increase of the available surface area of a single CubeSAT side by 136%. This is greater than that achieved by the CUTE-1 satellite fold-out design, which increases the available surface area by 100% [7] with a single fold-out panel. In determining these values, the surface area of the deployable calculation only considers the sun exposed side of the solar arrays on the single side of the cube involving the deployable. I.e., the single side of the cube is the baseline for calculations.

In addition to increased surface area, the circumferentially actuated design is expected to exhibit smooth deployment, is only 1 degree-of freedom, and provides for torque cancellation achievable via counter-rotation of the two rings simultaneously on

deployment. In terms of complexity compared to existing designs, the use of the Hoberman design eliminates the need for multiple spur gears, a DC motor, a gear head, and paddle stoppers by allowing for actuation by a single spring or motor [4,7]. While it is perceived that the multiple joints of the Hoberman mechanism add greater complexity, this can be simplified via using compliant joints or other large-strain joint configurations in the fabrication of the system.

Ballistic Drag Coefficient

Further considering that a maximum of two of these deployable mechanisms could be used at the same time on a given CubeSat, the Hoberman-based design can substantially increase the power generation capabilities of the CubeSAT. However, the increase in surface area also increases the ballistic drag coefficient (B) if the satellite is in a Low Earth Orbit (LEO, 500km-800km above the earth's surface). The drag coefficient (C_d) for a LEO is 2.2, and the mass of the satellite (m) will be approximately 1.2 kg. The projected drag area includes the area of one face of the satellite and the area of the deployed mechanism. The projected drag area is estimated to be 1.08×10^{-2} m^2, assuming the solar panels are deployed perpendicular to the orbit of the satellite. The ballistic drag coefficient is therefore,

$$B = \frac{m}{C_d A}$$

$$B = 50.51 kg / m^2$$

The ballistic drag coefficient for the current industry standard (CUTE-1 fold-out design) is 27.27 kg/m^2 [4]. The ballistic drag coefficient for the four panel fold-out design is 13.63 kg/m^2. As the value of B decreases, the time a satellite remains in orbit also decreases. In general, a satellite is required to remain in orbit for a given target time, which translates to a given target cross-sectional area. For picosatellites, the cross sectional areas and masses are so small that they have relatively high ballistic coefficients, which minimizes the impact to orbit. These results are tabulated in Table 1 for each of the designs. In addition, Figure 8 shows that the ballistic drag coefficient drops off approaching a constant value with an increase in the number of leaves selected for the Hoberman design . Similarly, the surface area available for solar arrays increases leveling off to a constant value with an increase in the number of leaves selected. Comparing the ballistic drag coefficient results with the increased area shows that potentially the trade off of shorter orbital life can yield greater power capacity of the small satellite. These would need to be weighed against the mission requirements of the small satellite to determine the optimal number of leaves.

Size, Stowed Volume, and Power Generation Analysis [4]

Table 1 contrasts the available surface area, power generation, and stowed volume for a base 1U CubeSat face. Stowed volume is calculated using an assumption that the

thickness of the solar panel mechanism being used is 1 cm in all cases. For design purposes, a factor of 0.85 is used to calculate the available surface area for solar panels after accommodating soldering, wiring, or any other constraints in mounting the solar arrays on the panel. In addition, it is assumed that power generation conditions are ideal (i.e., the solar panels are positioned perpendicular to the incoming sunlight). The solar panels on the presented design are shrunk to accommodate the rails on the edges of the CubeSat. This shrinkage may be minimized by removing the rails on the base side of the satellite, with an upper theoretical limit of a 300% increase in area. The total surface area available for solar panels is calculated as follows [4]:

$$N = 8 \text{ (number of panels)}$$

$$A_{base} = 100cm^2 \qquad A_{panel} = 17.1cm^2$$

$$A_{solar,base} = 0.85(100cm^2) = 85cm^2$$

$$A_{panel,base} = 0.85(17.1cm^2) = 14.5cm^2$$

$$A_{solar,total} = A_{solar,base} + N*A_{solar,panel}$$

$$A_{solar,total} = 85cm^2 + 8(13.6cm^2) = 201.3cm^2$$

Table 1: Surface Area, Power, Ballistic Drag Coefficient and Volume Trade Study

Description	**Surface Area When Deployed (cm^2)**	**Power (mW)**	**Ballistic Drag Coefficient (kg/m^2)**	**Stowed Volume (cm^3)**
*Base 1U CubeSat face	85.00	2125	54.54	20
CUTE-1 1U Fold-out [7]	170.00	4250	27.27	50
Circumferentially actuated deployable (1U)	201.30	5032	50.51	100
Four-Panel Fold-Out [4]	425.00	10625	13.63	140

* This design is not stowable and is included for reference only.

Alternate Designs

As discussed in in the above Solar Array Theoretical Development Section and the Ballistic Drag Coefficient Section, it is possible to change the available surface area by

changing the number of leaves of te mechanism while still maintaining the single degree-of-freedom system. Figure 8 [2] shows how the available surface area increases to a theoretical limit as the number of panels (n) increases. However, when considering the number of panels, one must also consider the added complexity of these designs which can exclude them from being viable alternatives at this stage of development.

Another design shown in Table 1 is the four-panel fold-out design. In this design, one panel folds out from each of the four sides attached to the base side, increasing the area by 400%. However, this design has 4 degrees of freedom. This alternative is a good option when maximum power is required for the CubeSat but is not advisable when trying to minimize shaking forces to the rest of the satellite during deployment. In addition, the deployment complexity when associated with the fold-out design is much larger than the deployment complexity for the Hoberman-based design presented in this thesis which requires only one single deployment release.

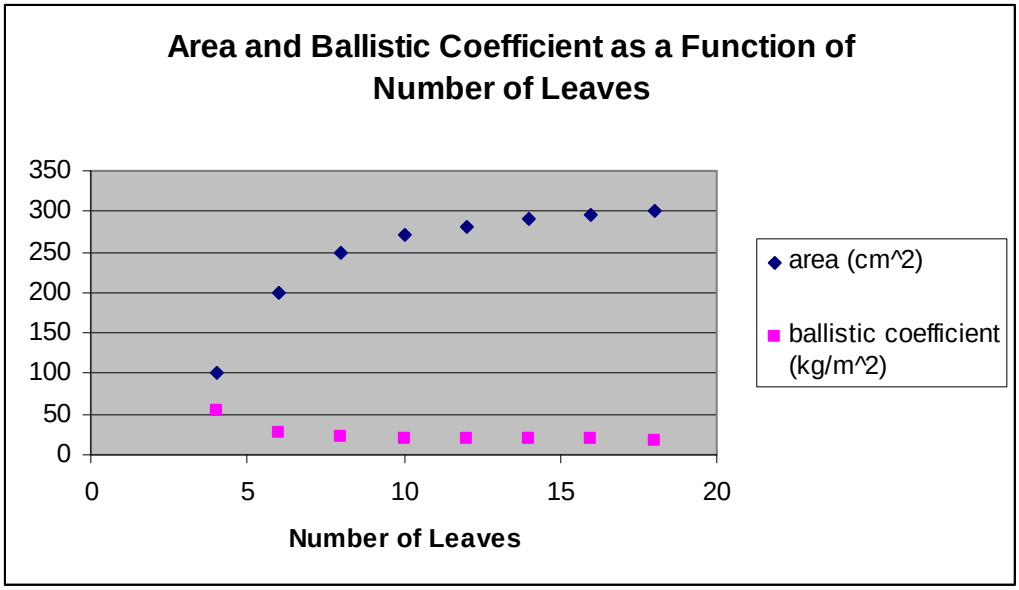

Figure 8. Available surface area and calculated ballistic coefficient versus number of Hoberman leaves.

Mounted Design

Figure 4 illustrates how the deployed mechanism is mounted on the CubeSat. The actuation is provided by a small drive spring, and the stowed mechanism fits within the envelope of the 1U CubeSat frame itself. Refer to reference [2] for greater detail on deployment actuation subsystem.

Part 3: Antenna Array Design

Antenna Array Theoretical Development

The most commonly recognized Hoberman mechanism is the collapsible sphere that is commonly used for a children's toy. Shown in Figure 9 in the stowed and deployed configuration of an 8-ribbed design, the basic sphere structure can be dissected to create a planar deployable spherical dish backbone with a prismatic (translational) form of actuation. The unit that is repeated to compose the structure of the dish consists of two ternary links that are joined at a common vertex B by a revolute joint, shown below in Figure 10. A necessary condition for mobility is that joints A, C, D, and E each have two degrees of freedom as a prismatic-revolute joint pair, thereby creating the PRRP linkages ABE and CBD with the common coupler point B that moves radially along line OB. In implementation, the mechanism becomes over-constrained, and thus each of the prismatic-revolute joint pairs can be replaced with a simple revolute joint between links while retaining the same radial motions. Revolute joints at points D and E for each backbone (rib) form revolute joints with the respective actuation octagons shown in Figure 9. The D's connect to the upper octagon and E's connect to the lower actuation octagon.

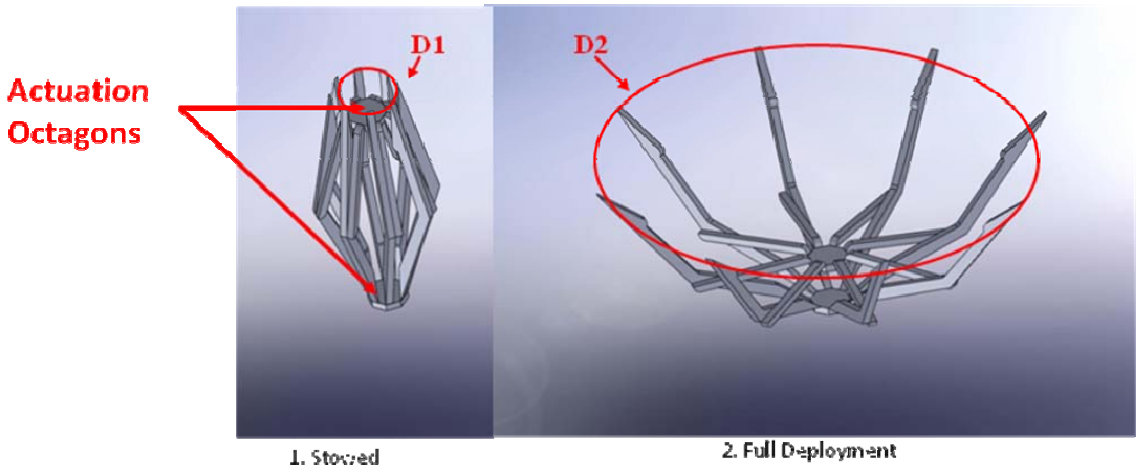

Figure 9: Deployed Octagonal Antenna Array Design

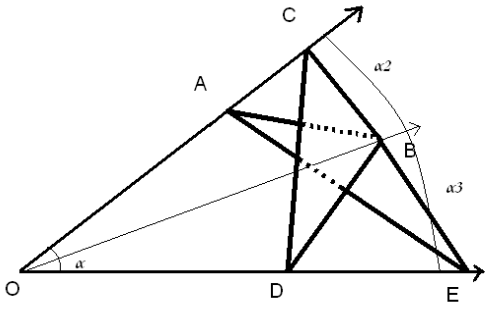

Figure 10: Two ternary links, ABE and CBD , with common coupler point B forming the basic sphere structure.

When the planar mechanism is packaged (stowed), it resembles a denser semi-circle. The planar case of the stowed mechanism is showed in Figure 11, and the planar case of the deployed mechanism is shown in Figure 12.

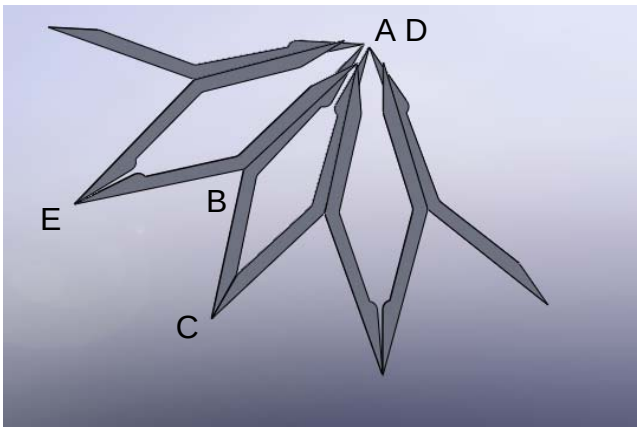

Figure 11: Stowed configuration of backbone's linkage.

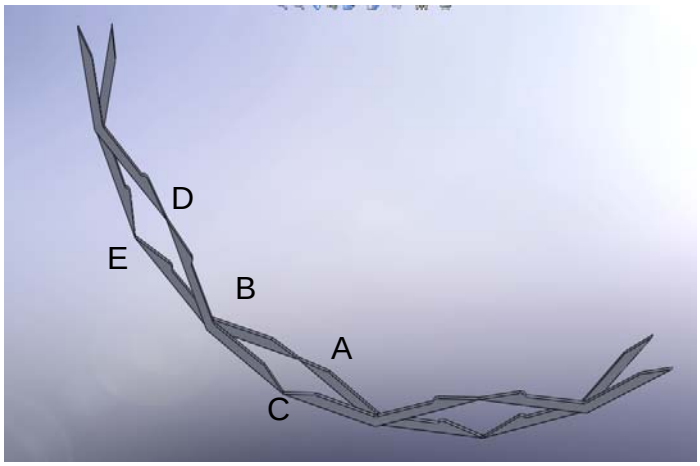

Figure 12: Deployed configuration of backbone's linkage.

This structure provides the backbone of the antenna dish. The surface composition of the dish is a subject that warrants future research, although the use of gold-plated molybdenum mesh is a promising option.

Antenna Array Performance Analysis

Antenna Gain

Because the antenna dish is spherical, not parabolic, the antenna can only achieve 80% of the gain performance of a corresponding parabolic antenna. However, this is shown not to be an issue of much concern due to the relatively high communications frequencies associated with small satellites. These frequencies tend to be around 2400 MHz. The equation for antenna gain (G) as a function of dish diameter (D) and signal wavelength (λ) is shown below. From this, it can be seen that the degree of expandability of the mechanism drastically influences antenna gain. In the following analysis, the following value is assumed for the signal wavelength (λ) equal to 0.125 m. The influence of the link lengths on the antenna gain is explored more in the below section on link length influence on diameter, gain, and far-field range.

$$G = \left(\frac{\pi \cdot D}{\lambda} \right)^2$$

Parametric Analysis of Expandability

Because the dish is not able to contract completely due to joint size limitations (refer to Figures 9 and 11), it is important to consider the extent of contraction/expansion of the mechanism. The expandability of the antenna dish is governed by the number of PRRP linkage pairs. The greater the number of PRRP linkages, the greater the amount of expansion/contraction of the mechanism [1]. However, as the number of linkages within the mechanism increases, the revolute joint size must also decrease to account for the increased compactness of the stowed arrangement. The farthest radial distance traveled by point B in Figure 10 is when the DB line becomes perpendicular to the horizontal axis which is equal to the maximum value of $DB/\sin\alpha_2$, where $\alpha_2=\alpha_3$ and the length of side DB equals the length of side EB.

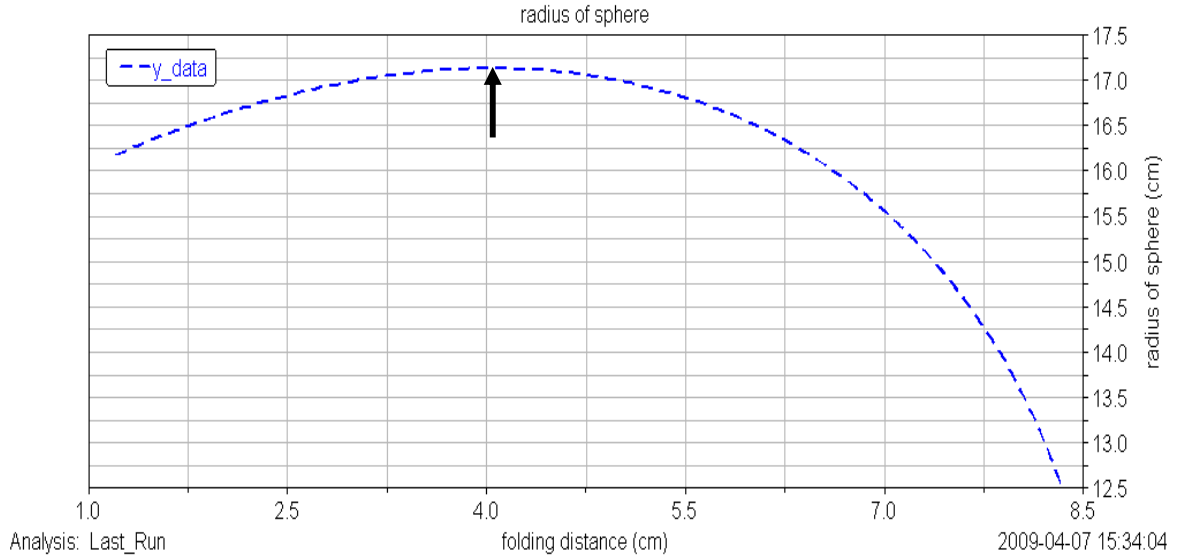

Optimal Folding Distance

The antenna design enables a 39% increase in the radius of the dish when fully deployed. The mechanism is actuated by means of a linear actuator. Figure 13 shows the external radius of curvature of the semi-sphere as a function of linear actuation. The variable that is labeled "folding distance" (defined in Figure 14) is a distance measurement that changes based on the amount of linear actuation. This distance is also the distance between the actuation octagons of Figure 9, the distance between DE of Figure 10. As can be seen by Figure 13, there is an optimum folding distance to obtain the maximum radius of the semi-sphere (maximum D2/2 in Figure 9). The sphere is at its maximum radius when the folding distance is approximately one half of the original folding distance. The original folding distance is d for stowed configuration where for design of Figure 13, d=8.4cm. The variable "folding distance" is labeled on the Figure 14, shown in its stowed configuration. When the folding distance is decreased, the sphere deploys, opens up. Determination of the maximum radius (or diameter D2) is significant because gain is proportional to the square of the dish diameter. Therefore the point of maximum dish diameter also equals the point of maximum antenna gain.

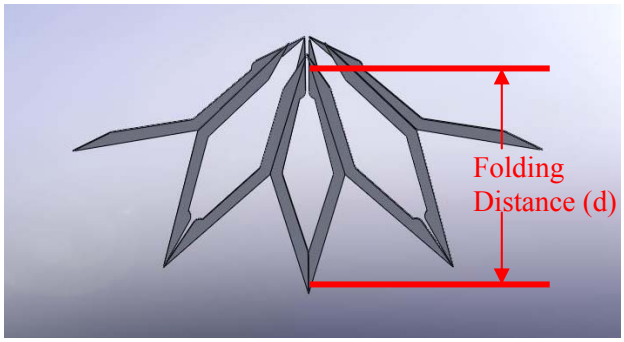

Figure 14: Folding distance of semi-sphere.

Extension of This Concept to Create an 8-Ribbed Design

As illustrated by Figure 9, the planar deployable dish design may be extended and modified to create a more stowable and practical 8-ribbed design. The eight rib pairs are arranged around two actuation octagons, which can be connected by a linear actuator such as a spring. Although eight ribs are shown in Figure 9, any number of ribs may be added to this design without any change in the above planar analysis because all ribs operate in parallel, actuated with the same actuator. As described above, the degree of deployment of the 8-ribbed design is a function of the folding distance variable (d). While the number of ribs does not affect the maximum potential gain of the structure directly (i.e., the radius functional relationship does not change with number of ribs), an increase in the number of ribs does provide greater control of the surface structure. The structural integrity (stability) of the antenna may have an indirect effect on the gain due to vibrational disturbances.

Influence of link length on antenna parameters (gain, far-field distance, diameter)

The link length that is being explored is of the link kinematic dimension defined as link L in Figure 15. Although L is only labeled once in the figure, each planar backbone mechanism has an identical link L due to symmetry (for the 8 ribbed antenna the total is 8). Link L was chosen for analysis because it has a large effect on the diameter (D2) of the deployed mechanism, yet it affects the mechanism in the least obvious way. The other, longer links can easily be physically shaped to alter the given shape of the mechanism when it is in its stowed or deployed configurations. This is an exciting aspect of this design in that the physical shape of the ribs can be altered to achieve a spherical or parabolic dish surface by defining the geometric shape of the extended branches of the (dimensions AB or CB of Figure 10). On the other hand, link L affects the movement of the mechanism during deployment as well as the final, deployed diameter (the length of link L does not have a large effect on the stowed volume).

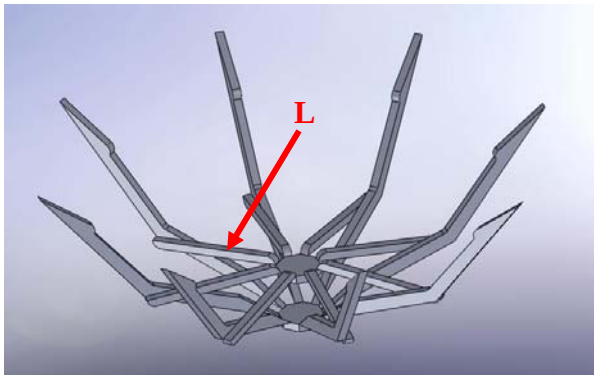

Figure 15: Identification of link L

As this link length is increased, the maximum potential diameter also increases. This change in diameter has an effect on the antenna characteristics of gain and far-field distance. Far-field distance (d_{ff}), also known as Fraunhofer distance, is defined below and is the distance from the antenna that defines the beginning of the far field region. The far field region is the region where the angular field distribution is essentially independent of the distance from the source (i.e., antenna).

$$d_{ff} = \frac{2D^2}{\lambda}$$

The effect of L on these parameters is shown below in Figure 16. As can be seen, all these antenna parameters increase exponentially as L increases. The upper limit of L is determined by the relative length of the longer links in the mechanism. Thus, if scaled by the other kinematic link length in the planar backbone mechanism, the overall size of the the reconfiguration driving components of antenna can be scaled. This component's size and the extended dimensions of AB or CB will both impact the resulting stowed volume of the antenna as well as the amount of gain achievable.

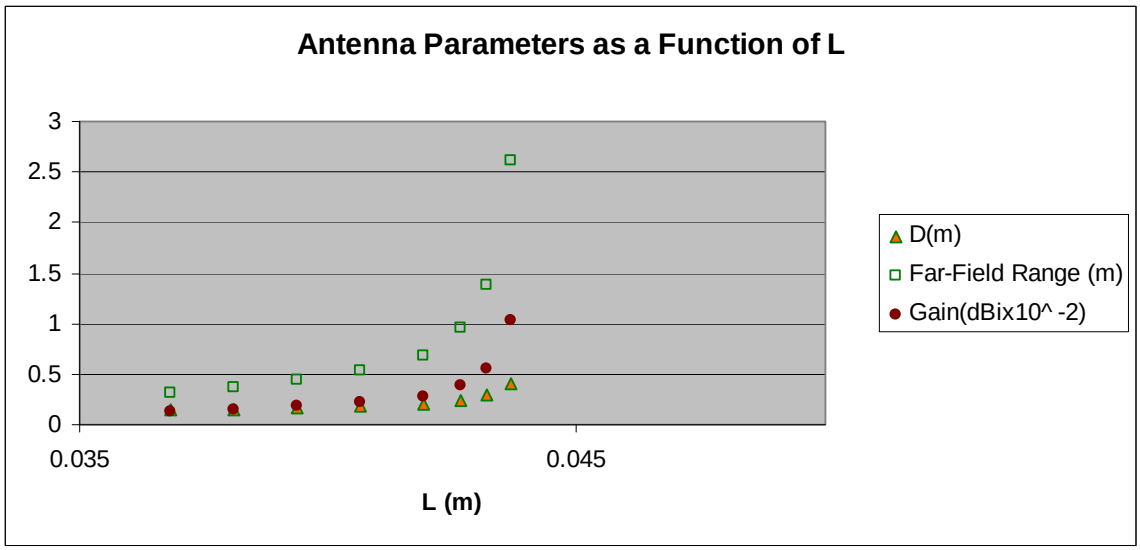

Figure 16: Antenna Diameter, Gain, and Far-Field Range as a function of link length L.

In the above calculations, it should be noted that the diameter used is the diameter of the circle approximating the reflectors equivalent spherical contour for given backbone structure as shown in Figure 17. This circle is defined by three points: the center of the center octagonal actuation link, and the two opposing vertices on the ends of the long links. For each value of L, the circle was calculated at the point of maximum dish expansion (or deployment).

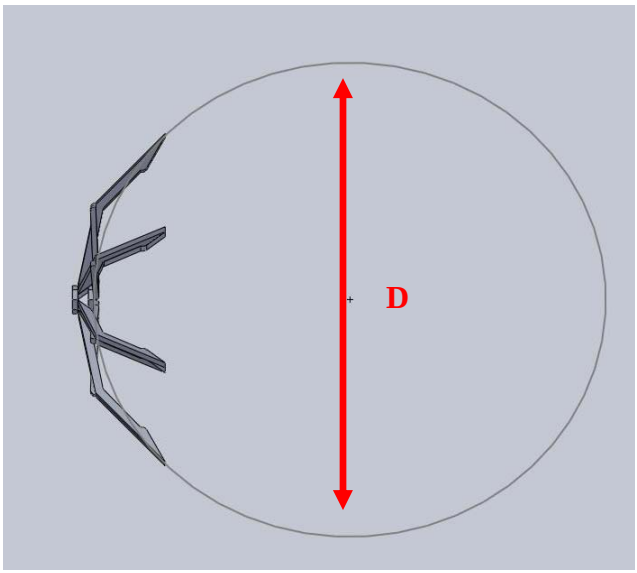

Figure 17: Definition of Dish Diameter

Part 4: Design Discussion

Discussion and Conclusions

In this thesis, the geometric and operational aspects of Hoberman based deployable solar arrays and dish antennas were presented. From the analysis of the decreased surface area and the increased ballistic factor of the presented design to the current state-of-the-art of fold out panels, the presented solar array design performs better than the fold-out panels. This benefit is compounded when considering 136% increase in surface area for power generation using the Hoberman based design compared to the 100% with the CUTE-1 fold out panel. Another benefit of the Hoberman-based design is that it only has a single degree-of-freedom and will impart minimal torque and shaking force on the small satellite, making this design preferable for missions with a high degree of attitude sensitivity. For the deployable antenna, the Hoberman kinematic theory provides a backbone that can be used to support a dish structure. The eight-ribbed deployable design has been explored, and this thesis presents a parametric study of the effect of link length on diameter, gain, and far-field distance. While the work presented in this thesis provides a methodology for analysis, design and evaluation of deployable solar arrays and antennas for small satellites, the specific power generation concept selection will still be heavily governed by the given orbit parameters and mission requirements.

In summary, the deployable nature of these single degree-of-freedom devices makes them viable alternatives to the current multiple degree-of-freedom deployable systems. The power generation capabilities of the deployable solar array have been demonstrated to yield a significant improvement over current methods of power generation for small satellites. In addition, the deployable dish design allows for enhanced communications capabilities while saving valuable stowage space.

Future Work

From this point, both the antenna design and the solar array design must be refined and tested for space conditions. Although these designs are kinematically viable for space applications, more analysis must be performed to make these designs dynamically and thermally ready for use on a small satellite.

References

[1] Jiten Patel and G.K. Ananthasuresh, "A Kinematic Theory for Radially Foldable Planar Linkages," International Journal of Solids and Structures, 44, 2007, pp. 6279-6298.

[2] James E. Roark, "Foldable Mechanism to Improve the Functionality of Small Satellites", University of Florida, Department of Mechanical and Aerospace Engineering, Undergraduate Honors Thesis, May 2009.

[3] Wiens, G.J., Umsrithong, A. Miller, S., Koka, A. and Vitello, T., "Design of Autonomous Foldable Docking Mechanism for Small Space Vehicles", Proceedings of International Design Engineering Technical Conferences, DETC2009-87678, San Diego, CA, August 30-September 2, 2009, 12 pp.

[4] Wiens, G., McNair, J., Miller, S., Rao, K., Brandt, K., Obulapathi, C., Muri P., Faist, K., and Roark, J., "Deployable Mechanisms For Small Satellites (DMSS)", Conceptual Design Report – Lockheed Martin Corporation, LMC PO# RRMJS6769, UF Contract No.: 00071765, June 26, 2009, 64 pp.

[5] Robert L. Norton, "Design of Machinery, 4th Edition", McGraw-Hill, 2008.

[6] http://cubesatkit.com/, October 10, 2009.

[7] http://lss.mes.titech.ac.jp/ssp/cubesat/index_e.html, October 19, 2010.

[8] Nakaya, Koji "Tokyo Tech CubeSat: CUTE-I"

[9] Krishnamurthy, Narayanan "Dynamic Modeling of CubeSat Project MOVE" 2008

[10] Fujishige, Timothy S. "Active Antennas for CubeSat Applications" USU Conference on Small Satellites